

## OPTIMISATION OF HEAT TRANSFER IN NON-NEWTONIAN FLUIDS WITH CHAOTIC ADVECTION

Daniel R. Lester<sup>1</sup>, Murray Rudman<sup>1</sup>, Guy Metcalfe<sup>1</sup>

<sup>1</sup> CSIRO Manufacturing and Materials Technology, Highett, Victoria 3190, AUSTRALIA

### ABSTRACT

Temperature control in the pharmaceutical, food, and mineral processing industries is complicated by the inherent rheological complexity of the materials involved. For example, food sterilization requires uniform heating of typically non-Newtonian foodstuffs within a narrow temperature range. Despite complex rheology, the enhanced transport characteristics of laminar flows exhibiting Lagrangian chaos can address these requirements. Flow behaviour as such is controlled by a number of device design and operating parameters, generating an optimisation problem over these parameters. This problem is difficult as the parameter space may be large and the solution distribution complex (fractal). By developing a novel spectral method, we can resolve the asymptotic heat transfer rate over the entire control parameter space, solving the optimization problem. This method is applied to a case study of a Hershel-Bulkley fluid in the Rotated Arc Mixer, where a 6-fold increase of heat transfer occurs at Peclét number  $Pe=10^3$ , which increases with  $Pe$ .

### INTRODUCTION

Ubiquitous to the food, pharmaceutical and mineral processing industries are non-Newtonian materials such as emulsions, suspensions, slurries and pastes. Due to this rheological complexity, transport and processing of such materials involves unique difficulties, especially for delicate, high viscosity, yield stress and/or viscoelastic materials. Furthermore, very often such processes or materials are temperature sensitive; for example food sterilization demands uniform heating of shear and temperature sensitive foodstuffs within a narrow temperature range, and reaction of biological agents, demands precise temperature control to inhibit unwanted side reaction due to the specific activation energies involved. As conduction and natural convection alone are generally insufficient to achieve the required heat transfer rate for uniform temperature distribution, forced convection of the material is required to enhance heat transport. However, traditional approaches such as the introduction of turbulence are often not feasible for non-Newtonian materials due to large energy costs, high apparent viscosities, and the often shear-sensitive nature of these materials. As heat transfer enhancement via forced convection does not occur within plug flow regions inherent to yield stress materials, a further consideration involves ensuring material elements do not solely reside within such regions. With these considerations in mind, a promising method to enhance transport characteristics of non-Newtonian materials whilst addressing these requirements is chaotic

advection, whereby chaotic fluid particle paths arise from a velocity field which may be non-turbulent. Lagrangian chaos can be achieved even within Stokes flow and so is attractive for processing of non-Newtonian and shear-sensitive fluids.

While chaotic advection directly enhances transport of passive entities (i.e. mixing of tracers), these principles also apply to dissipative systems, e.g. the transport of diffusive particles or heat. In such cases the optimum mixing protocol differs from that of the non-diffusive system. Due to complex interaction between the kinetic advection and dynamic molecular transport processes, the fundamentals of chaotic advection-diffusion are not fully understood, however the potential benefits of such phenomena are large. Practically, what is the magnitude of these benefits, and how can we exploit them?

Chaotic advection devices involve a number of variable design and operating parameters which must be optimised for the process at hand. For pure mixing, global chaos is desirable, whereas for other applications (e.g. mixing and reaction), different protocols may be preferred. For diffusive mixing, the relative timescales of advection and diffusion must be accounted for. In all but very trivial flows, the optimum set of control parameters cannot be determined analytically, so experimental or numerical investigation is required. The control parameter space can be large, and results herein suggest the process efficiency has a complex (fractal) distribution with multiple local maxima, so high resolution global exploration of this space is required to confidently identify the global optimum. Until recently, the computational overhead of exploring the control parameter space to sufficient resolution has been prohibitive. This has hindered optimisation of enhanced transport devices based upon chaotic advection.

Diffusive entities are active scalars, however very often the fluid velocity field is independent of the scalar distribution, in which case they are considered passive and diffusive. In the case of heat transfer, this corresponds to negligible effects of buoyancy, surface tension and viscosity change with temperature, and under such conditions, a novel spectral method (the *composite spectral method*, Lester et al, 2006a) which exploits the symmetries of chaotic flows is applicable. This method can rapidly explore the control parameter space to high resolution in terms of the so-called *strange eigenmodes* (Liu and Haller, 2003) of the advection-diffusion equation (ADE) governing scalar transport. In the case of

periodic advective velocities the strange eigenmodes manifest as exponentially decaying periodic patterns. Eventually the slowest decaying strange eigenmode dominates, and so the asymptotic transport characteristics are governed by this eigenmode. As such, transport characteristics may be inferred from the dominant strange eigenmode dynamics rather than the full solution of the scalar advection equation, facilitating rapid exploration of the control parameter space.

Previously this method has been used (Lester et al, 2006b) to explore the control parameter space of the 2D analogue of a chaotic mixing device, the Rotated Arc Mixer (RAM) (Metcalf et al, 2006), processing a Newtonian fluid. As the 3D RAM is more industrially relevant due to its simple design and ability to process fluids in a continuous fashion, we consider this device here. The former study involves analysis of a temporally periodic 2D system, whilst this study considers a spatially periodic steady 3D system. We consider heat transfer of a shear-thinning yield stress fluid in the RAM, as such materials are commonly encountered in the process industries which are particularly problematic as the plug flow regions inherent to yield stress fluids present natural barriers to transport.

The aim of this work is to quantify and optimize heat transfer of a non-Newtonian fluid in the RAM with respect to a suitable reference, and investigate qualitative characteristics of the chaotic advection diffusion system over the control parameter space. As temperature homogenization is generally of primary concern for heat sensitive fluids in industry, we only consider the fixed flux mode of operation, which also captures the same physics as the mixing of diffusive species.

The geometry, control parameters and governing equations are outlined in Section 2, and the solution methods are reviewed in Section 3. Results and conclusions are covered in Sections 4 and 5 respectively.

## PROBLEM DEFINITION

A detailed description of the Rotated Arc Mixer illustrated in Fig. 1 is given in Metcalfe et al (2006), and Fig. 2 depicts the RAM parameters. In brief, the RAM consists of an inner cylinder of inner radius  $R$  through which the fluid flows, and tightly wrapped around this is an outer cylinder which rotates at fixed angular velocity  $\Omega$ . Regular apertures are cut into the inner cylinder of arc angle  $\Delta$  and length  $L$ , such that at the end of one aperture, another is added immediately afterwards, offset by angle  $\Theta$ , resulting in a reoriented duct flow. Rotation of the outer cylinder imparts transverse flow to the fluid on top of the axial flow along the inside of the inner cylinder, and so each ‘‘cell’’ of the RAM corresponding to an aperture experiences a combination of these axial and transverse flows. From cell to cell, this basic flow is simply reoriented by the offset angle  $\Theta$ . If  $U$  denotes the average axial velocity, then the ratio of timescales between the axial to transverse velocities is defined as

$$\beta = \frac{\Omega L}{U}. \quad (1)$$

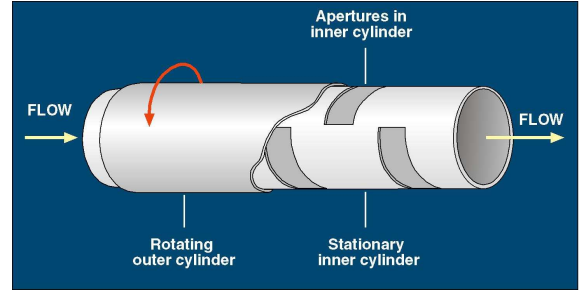


**Figure 1:** Rotated Arc Mixer schematic

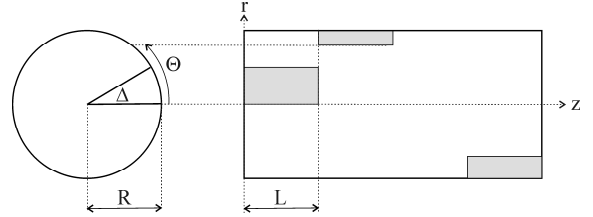


**Figure 2:** Rotated Arc Mixer parameters

The set of 3 flow control parameters  $\beta$ ,  $\Delta$ ,  $\Theta$  determine mixing conditions within the RAM, along with the usual rheological, inertial, and surface parameters. Diffusion introduces a control parameter quantifying the timescale between advection and diffusion, namely the Peclet number,  $Pe$ , which scales linearly with rotation rate  $\Omega$ :

$$Pe = \frac{V_0 L_0}{D_0} = \frac{\Omega R^2}{D_0}. \quad (2)$$

$D_0$  is thermal diffusivity and  $V_0$ ,  $L_0$  are the characteristic transverse velocity and length scales.

Under conditions that temperature acts as passive diffusive scalar, the momentum transport (Navier-Stokes) equation is independent of the heat transport (advection-diffusion) equation. To solve the fluid velocity field, we invoke the ‘‘two and a half dimensional’’ approximation of Metcalfe et al (2006), which in essence treats the flow field in each cell as two-dimensional; consequently the transition flows at cell boundaries are ignored. For Newtonian fluids, the relative thickness of this transition region is negligible for  $Re < 10$ , and so the RAM velocity field is also considered piecewise constant in  $z$  here. The extra ‘‘half dimension’’ above refers to the fact that the transverse and axial flows are coupled via the rate dependant non-Newtonian viscosity (Speetjens et al 2006). We need only determine the velocity field in the first cell,  $\mathbf{v}(r, \theta)$ , and from the 2.5D model, the full RAM velocity field  $\mathbf{u}(r, \theta, z)$  is mapped as

$$\mathbf{u}(r, \theta, z) = \mathbf{v}\left(r, \theta - \Theta \sum_{k=1}^{\infty} H(z - kL)\right), \quad (3)$$

where  $H$  is the Heaviside step function. For rational values of  $\Theta/\pi$ , the fluid velocity  $\mathbf{u}$  is  $z$ -periodic with periodicity  $jL$  for some integer  $j$ . Shear dependence of the non-Newtonian rheology results in coupling between the axial  $v_{r,\theta}(r, \theta)$  and transverse  $v_z(r, \theta)$  velocities, and the steady, incompressible, non-buoyant flow is driven by both the rotating outer sleeve and a constant axial pressure gradient  $C_p$ , such that the total pressure  $p$  is of the form  $p = P(r, \theta) + C_p z$ . The cell velocity  $\mathbf{v}$  is governed by the continuity and Navier-Stokes equations

$$\nabla \cdot \mathbf{v} = 0, \quad (4)$$

$$\rho \mathbf{v} \cdot \nabla \mathbf{v} = \nabla \cdot (2\eta \boldsymbol{\sigma}) - \nabla p, \quad (5)$$

where  $\boldsymbol{\sigma} = \frac{1}{2}(\nabla \mathbf{v} + (\nabla \mathbf{v})^T)$  is the rate of deformation tensor,  $\dot{\gamma} = \sqrt{2\boldsymbol{\sigma} : \boldsymbol{\sigma}}$  the shear strain rate, and  $\rho$  the fluid density.  $\eta(\dot{\gamma})$  is the fluid viscosity, given by the Hershel-Bulkley (HB) model, with shear yield stress  $\tau_y$ , fluid consistency  $\kappa$ , and flow index  $n$ :

$$\eta(\dot{\gamma}) = \frac{\tau_y}{\dot{\gamma}} + \kappa \dot{\gamma}^{n-1}. \quad (6)$$

The fluid temperature  $\phi(\mathbf{x})$  over the RAM is governed by the steady advection-diffusion equation (ADE)

$$\mathbf{u} \cdot \nabla \phi = D_0 \nabla^2 \phi + f(\mathbf{x}), \quad (7)$$

subject to the boundary conditions

$$\phi(r, \theta, 0) = \phi_0(r, \theta) - \langle \phi_0(r, \theta) \rangle, \quad (8)$$

$$\left. \frac{\partial \phi}{\partial r} \right|_{r=R} = g(\theta, z), \quad (9)$$

where  $f$ ,  $g$ , respectively are the domain and boundary source terms. As the ADE (7) is linear, we only consider initial conditions (8) with zero mean without loss of generality. Non-dimensionalisation of the ADE (7) follows from the scalings  $r' = r/R$ ,  $z' = z\Omega/U$ ,  $u_z' = u_z/U$ ,  $u_{r,\theta}' = u_{r,\theta}/(\Omega R)$ , and substitution (upon dropping primes) gives the non-dimensional heat transport equation

$$u_z \frac{\partial \phi}{\partial z} = -\mathbf{u}_{r,\theta} \cdot \nabla_{r,\theta} \phi + \frac{1}{Pe} \nabla_{r,\theta}^2 \phi + \frac{1}{\Omega} f(\mathbf{x}), \quad (10)$$

where the axial convection term  $\Omega^2/(Pe U^2) \partial^2 \phi / \partial z^2$  is ignored under the assumption that  $L \approx R$  and due to the transverse velocity, transverse temperature gradients dominate over axial gradients. In cases where this term is significant, with minor modification (extension to a nonlinear eigenproblem) the method is still applicable.

## METHOD

Maximisation of heat transfer in the RAM represents an optimisation problem over the control parameter set  $\{\Delta, \Theta, \beta, Pe\}$  for a given rheology. The set of design and operating parameters for the RAM form a four-dimensional space which govern the heat transfer characteristics of the device. Following previous investigations (Metcalf et al 2006), we only consider  $\Delta = \pi/4$  here, although it is understood different values of  $\Delta$  may be preferential for HB rheology. Previous studies (Lester et al 2006a, 2006b) also indicate that when optimised, transport enhancement increases significantly with  $Pe$ , and so only a moderate Peclet number ( $Pe = 10^3$ ) is considered here. As the cell velocity  $\mathbf{v}$  is independent of the remaining parameters  $\beta$ ,  $\Theta$ , the Navier-Stokes equations need only be solved once over the relevant control parameter space, and the RAM velocity field  $\mathbf{u}$  can subsequently be constructed via (3) for any choice of  $\beta$  and  $\Theta$ .

The 2D steady Navier-Stokes equations (4), (5) are numerically solved using the commercial CFD package

CFX-10<sup>®</sup>, for a HB fluid with yield stress  $\tau_y = 20$  Pa, consistency  $\kappa = 20$  Pa s<sup>0.5</sup>, flow index  $n = 0.5$  flowing in a RAM cell of radius  $R = 0.05$  m, driving axial pressure gradient  $C_p = 2000$  Pa m<sup>-1</sup>, window opening  $\Delta = \pi/4$ , and outer sleeve rotation rate  $\Omega = 1$  Hz. A series of increasing refined meshes is used to establish convergence and accuracy of the solution. To ensure incompressibility is satisfied exactly, the cell velocity is exported as  $\mathbf{v} = \hat{\mathbf{z}} \times \nabla \Psi + v_z$  where  $\Psi$  is the transverse flow streamfunction. This formulation allows computational savings when analysing scalar transport.

Solutions of the ADE (equation 10) may be cast in terms of strange eigenmodes, which in essence are the Floquet modes of the periodic steady 3D system (the dimensionless RAM velocity is  $\beta j$ -periodic in  $z$ ). Liu and Haller (2003) have established existence and convergence of these solutions, providing mathematical basis for decomposition of solutions of the ADE into a *finite* number of superimposed strange eigenmodes and an arbitrarily small fast-decaying non-eigenmode term. As such, the dimensionless temperature field may be represented as

$$\phi(\mathbf{x}) = \sum_{k=0}^K \alpha_k \phi_k(\mathbf{x}) e^{\lambda_k z} + \mathcal{O}(e^{-\rho z}), \quad (11)$$

where  $\phi_k(\mathbf{x})$  is the  $k$ -th strange eigenmode (which is  $\beta j$ -periodic in  $z$ ),  $\lambda_k$  is the associated decay rate,  $\alpha_k$  is the weighting due to the initial condition  $\phi_0$ , and the final term is the non-eigenmode contribution. With time, the slowest decaying eigenmode dominates and so the asymptotic system dynamics may be approximated by this eigenmode;

$$\phi(\mathbf{x}) \rightarrow \phi_\infty(\mathbf{x}) = \alpha_0 \phi_0(\mathbf{x}) e^{\lambda_0 z}, \quad (12)$$

and so  $\lambda_0$  governs the lengthscale of asymptotic decay. Strange eigenmodes may also be complex, the pattern in which case has spatially quasiperiodic or subharmonic eigenmodes, depending upon whether  $\text{Im}(\lambda_k)$  is rationally related to  $2\pi\beta$ . For any initial condition given  $\alpha_0 \neq 0$ , the same eigenmode dominates, and in this study we concentrate solely on the dominant strange eigenmode only, under the assumption that  $\alpha_0 \neq 0$ . Indeed, it is generally true that  $\alpha_0 > \alpha_k$  for all  $k$  as the majority of initial data is projected onto the most regular (i.e. lowest total variance) eigenmode, which Liu and Haller (2003) show to be the dominant strange eigenmode. If  $\alpha_0 = 0$  or the short time dynamics are of interest, it is necessary to compute the leading few strange eigenmodes. When inhomogeneous boundary or source terms are present, solution of the ADE involves forcing terms which decay in terms of the strange eigenmodes

$$\phi(\mathbf{x}) = \sum_{k=0}^K \left( \alpha_k + \int_0^z F_k(u) du \right) \phi_k(\mathbf{x}) e^{\lambda_k z}, \quad (13)$$

where  $F_k(z)$  is the contribution of the source terms  $f(\mathbf{x})$ ,  $g(\mathbf{x})$  to the  $k$ -th strange eigenmode. Strange eigenmodes still govern decay of the system toward equilibrium, at a rate again dictated by the dominant eigenmode decay rate  $\lambda_0$ . Therefore the dominant strange eigenmode quantifies heat transfer in the RAM irrespective of initial conditions and source terms, and the optimal operating condition is

universal. Henceforth boundary and domain source terms are ignored.

The composite spectral method (Lester et al 2006a,b) rapidly calculates the strange eigenmodes of the unsteady advection diffusion equation with time-periodic advective velocity. With minor modification, this method can also be applied to the steady ADE (10) with spatially periodic advective velocity. In essence, the axial coordinate  $z$  replaces time, and the formulations would be identical if the axial velocity  $u_z$  were plug flow. Spectral expansion and truncation of (10) in terms of Laplacian eigenfunctions with appropriate boundary conditions results in the system

$$\mathbf{B}(z) \frac{d\Phi}{dz} = \left( \mathbf{H}(z) - \frac{1}{Pe} \mathbf{D} \right) \Phi, \quad (14)$$

where  $\mathbf{B}(z)$  is the operator matrix for the axial velocity,  $\mathbf{H}(z)$  is the operator matrix for the transverse advection term, and  $\mathbf{D}$  is the constant operator matrix for the diffusion term. As  $\mathbf{B}(z)$  and  $\mathbf{H}(z)$  are both piecewise constant in  $z$ , the system can be recast as

$$\frac{d\Phi}{dz} = \mathbf{B}(z)^{-1} \left( \mathbf{H}(z) - \frac{1}{Pe} \mathbf{D} \right) \Phi = \mathbf{A}(z) \Phi, \quad (15)$$

and so analysis proceeds as in Lester et al (2006a,b).

The aim of this study is to solve for the dimensionless dominant strange eigenmode  $\phi_0(\mathbf{x})$  and associated decay rate  $\lambda_0$  of the heat transfer equation (10) over the parameter space  $\mathbf{Q}: \{\beta, \Theta\} = [-\pi, \pi] \times [0, \infty]$ , at  $Pe=10^3$  and quantify the heat transfer enhancement. To do so, we compare heat transfer in the RAM against the reference case of heat transfer for simple pipe flow, specifically that for the same fluid flowing with the same mean axial velocity  $U$  in a pipe of the same dimensions as the RAM. As such, heat transfer enhancement in the RAM can be correlated with the energy difference associated with driving of the transverse flow and different axial pressure gradients. For the HB rheology (6), the radially dependant axial velocity  $u_z(r)$  has an analytic form, where an axial pressure gradient of  $C_p=3940.37 \text{ Pa m}^{-1}$  matches the axial mean flow  $U$  to that of the RAM flow. Ignoring axial diffusion, and assuming axisymmetry, the heat transport equation for simple pipe flow is

$$u_z(r) \frac{\partial \phi}{\partial z} = \frac{1}{Pe} \nabla_r^2 \phi, \quad (16)$$

subject to boundary conditions (8), (9). As such the asymptotic (long  $z$ ) temperature decays as  $\exp(\xi_0 z/Pe)$ , where  $\xi_0$  is the lowest magnitude eigenvalue of the operator  $\nabla_r^2 / u_z(r)$ . In comparison, the dominant strange eigenmode in the RAM decays as  $\exp(\lambda_0 z)$ , hence the heat transfer enhancement factor  $q$  which quantifies the relative lengthscales of asymptotic heat transfer is

$$q \equiv \frac{\text{Re}(\lambda_0) Pe}{\xi_0}. \quad (17)$$

In practical terms a simple pipe heat exchanger needs to be  $q$  times longer to achieve the same level of heat transfer as the RAM. Once the relative energy expenditure of the RAM and distribution of  $q$  over the

control parameter space  $\mathbf{Q}$  are known, we can quantify the level and cost of optimised heat transfer in the RAM.

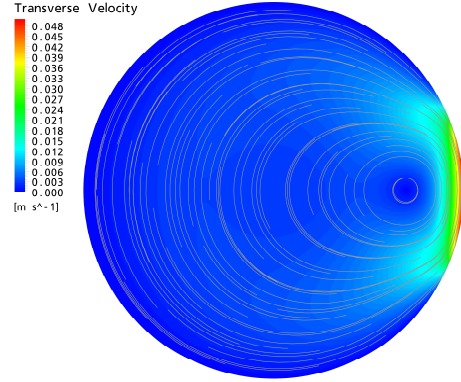


**Figure 3:** RAM cell transverse velocity profile and streamlines

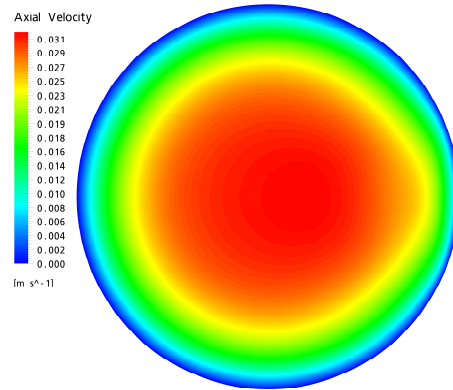


**Figure 4:** RAM cell axial velocity profile

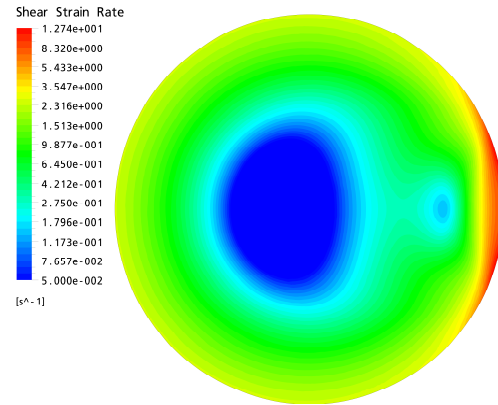


**Figure 5:** RAM cell shear strain rate

## RESULTS

The CFD results for the 2.5D cell model are shown in Fig. 3-5. The cell window is located at 3 o'clock, where the highest transverse velocity occurs. The cell centre and the centre of the circulation region (Fig. 3), are barriers to transport enhancement as the local shear rate is zero; however the angular offset  $\Theta$  between cells means that fluid elements may experience shear in subsequent cells. The results in Fig. 3-5 are the basis for construction of the full RAM velocity field  $\mathbf{u}$ , as parameterised by  $\Theta$  and  $\beta$ . Coupling of the axial and transverse flows via the non-Newtonian viscosity is apparent in Fig. 4, where the angular asymmetry arises

from shear thinning of the fluid near the aperture window. A plug flow region occurs to the right of the cell  $r=0$  axis, and so the angular offset between cells is capable of moving fluid elements out of this plug region. From the CFD results, the work per unit length required to drive the outer sleeve of the RAM is  $0.8927 \text{ W m}^{-1}$ , which in addition to the axial pressure gradient gives a total of  $1.2330 \text{ W m}^{-1}$ . In comparison, a work per unit length of  $0.6644 \text{ W m}^{-1}$  is required to drive the pipe flow, so the RAM flow requires roughly double the energy input. The shear thinning nature of the HB fluid means that the transverse work done by the rotating outer sleeve reduces the work required to axially drive the fluid, and this phenomenon is common as most pseudo-plastic fluids are shear thinning.

For the base case of heat transfer under simple pipe flow, the dominant eigenfunction for the operator  $\nabla_r^2 / u_z(r)$  is calculated by spectral analysis, in a similar fashion to the calculation of the RAM strange eigenmodes for the ADE (10), with the simplifications that the analysis is 1D, and the axial fluid velocity  $u_z(r)$  is of analytic form. We find the corresponding eigenvalue to be  $\zeta_0 \approx 7.5238$ , which is the lengthscale (in  $z$ ) of asymptotic heat transfer for the HB fluid under simple pipe flow, which can now be compared to that of the RAM.

The dominant strange eigenmode  $\varphi_0(\mathbf{x}, t)$  and associated decay rate  $\lambda_0$  for fixed flux (Neumann) boundary conditions is determined using the spectral method of Lester et al (2006a,b) over the parameter space  $\mathbf{Q}:\{\beta, \Theta\} = [-\pi, \pi] \times [0.02, 500]$ , at  $Pe=10^3$ , with  $q$  calculated and plotted in Fig. 6. This plot has around  $1.7 \times 10^5$  points (where the dominant strange eigenmode and associated decay rate are determined at each point), and the total computation required  $2.76 \times 10^5$  seconds on an Intel® Xeon™ 3.00 GHz CPU. In contrast, using the same

processor, numerical solution of the ADE *only* for a single point in  $\mathbf{Q}$  to similar accuracy (to verify results of the spectral solution) using the CFD software CFX 10.0™ for  $z$  large enough to observe  $\lambda_0$  requires  $2.3 \times 10^5$  seconds of computation. As such the spectral method is around 14,000 times faster in this instance; it is this computational efficiency which facilitates detailed exploration of the RAM control parameter space.

The heat transfer enhancement distribution here is of similar complex (fractal) structure to that of a Newtonian fluid in a 2D RAM with Neumann boundary conditions (Lester et al 2006). Again, ridges of enhanced  $q$  (Arnol'd tongues) emanate from the  $\beta=0$  axis at rational values of  $\Theta/\pi$ . Prior to collision of these tongues around  $\beta=5$ , the strange eigenmodes are ordered, and rotationally symmetric on the Arnol'd tongues, as depicted in Fig 7 (a)-(c). The large gradients maintained in these “programmed” structures result in enhanced transport; however, off the tongues (Fig. 7(d)) the rotational symmetry is lost and heat transfer enhancement is minimal ( $q=1.679$ ). Enhancement also occurs in the case of no reorientation ( $\Theta=0$ , Fig. 7(e)), but not to the same degree as in the dominant Arnol'd tongues. A disorder transition occurs around  $\beta>5$ , resulting in greater transport enhancement than the ordered solutions. The eigenmodes at characteristic points within  $\mathbf{Q}$  are shown in Fig. 8. There exist several regions of *locally* optimal enhancement within  $\mathbf{Q}$ , all of which are large enough to be considered parametrically robust. In contrast to the ordered solutions (Fig. 7), the patterns associated with these local optima ((f), (g), (i)) do not exhibit evidence of solid body conduction associated with the plug flow region (Fig. 5) of the HB fluid. As such, appropriate cell reorientation in the RAM flow is capable of transporting fluid elements (and hence heat) out of this region.

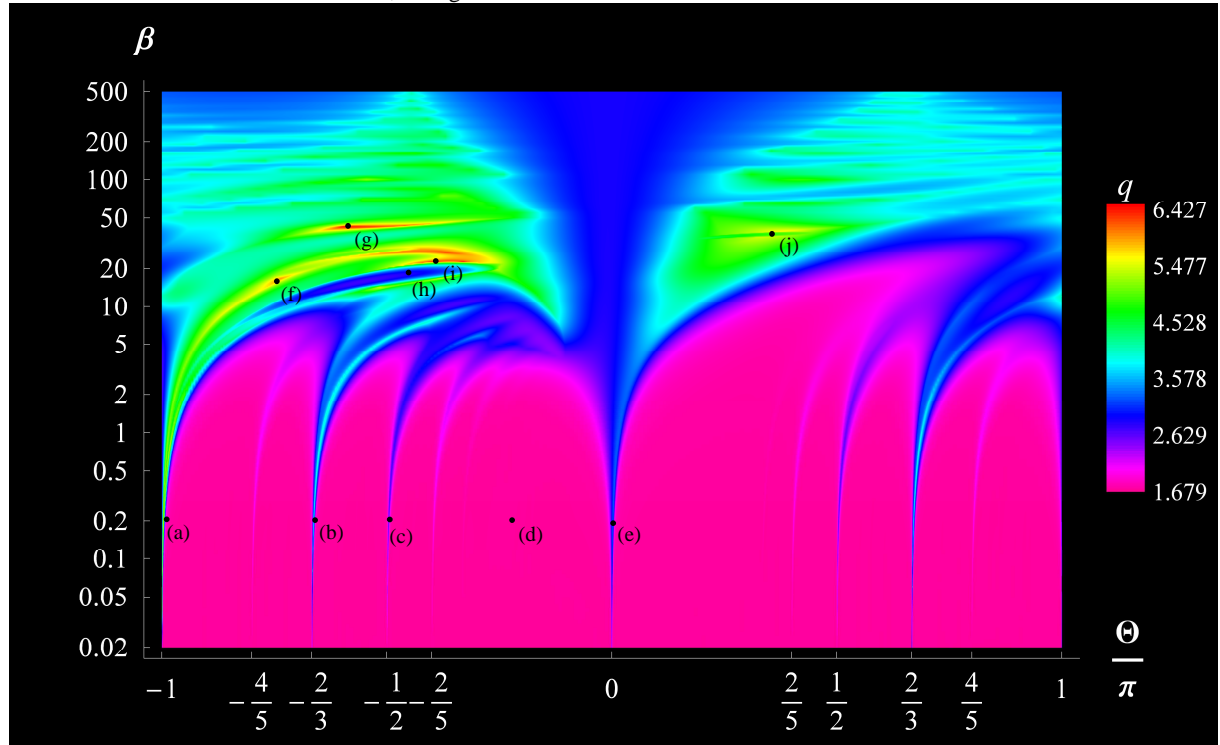


**Figure 6:** Heat transfer enhancement  $q$  over  $\{\beta, \Theta\}$  space for  $Pe=10^3$ .

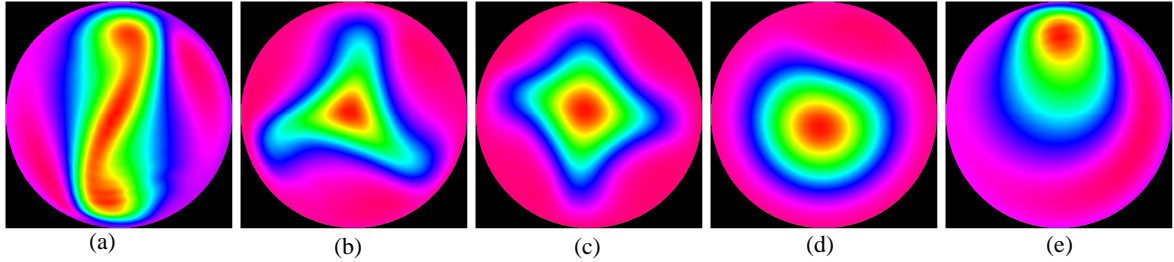


**Figure 7:** (a)-(c): Symmetric strange eigenmodes on Arnol'd tongues at  $\beta=0.2$ , (d), (e): non-symmetric eigenmodes at  $\beta=0.2$

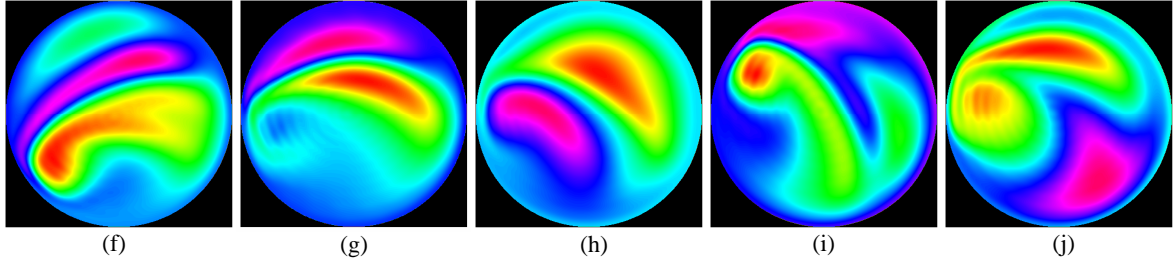


**Figure 8:** Disordered strange eigenmodes over RAM parameter space  $\mathbf{Q}$ , (i) corresponds to optimum heat transfer.

The global optimum over  $\mathbf{Q}$  occurs at point (i) (Fig. 8(i)), where the heat transfer is enhanced more than 6-fold ( $q_{\max}=6.427$ ) over the reference case. The significant enhancement means that based upon asymptotic behaviour, a pipe over 6.4 times the length of the RAM is required to achieve the same transfer of heat. As energy consumption of these devices scales with axial length, to achieve the same heat exchange, the RAM actually requires only 28.9% of the energy!

It is clear from Fig. 6 that detailed exploration of  $\mathbf{Q}$  is necessary to find this optimum. As the physics of heat transfer with insulated boundary conditions is analogous that of the mixing of passive diffusive species, we expect that protocols which produce good mixing (in the absence of diffusion) also correspond to enhanced heat transfer. We note that the region of enhanced transport within  $\mathbf{Q}$  corresponds roughly (but not exactly) to that of good mixing of Newtonian fluids in the RAM (Metcalf et al 2006).

## CONCLUSIONS

In this study we have applied a novel spectral method (Lester et al 2006a) to solve the asymptotic dynamics of heat transfer within a Herschel-Bulkley fluid over a subspace  $\mathbf{Q}$  of the control parameter space of a chaotic flow, the RAM flow. The heat transfer enhancement has been calculated against the reference of the same fluid flowing axially within a similar pipe. We find transport rate distribution to be complex (fractal), necessitating high resolution of  $\mathbf{Q}$  to identify the global optimum, and study the global structure of transport in this system. The transport rate distribution over the control parameter space shares many qualities with that of previous studies for Neumann boundary conditions (Lester et al, 2006b).

The optimised RAM has a greater than 6-fold acceleration of heat transfer at  $Pe=10^3$ , and only requires 29% of the energy to achieve the same heat exchange as the reference case. Based on previous results (Lester et al 2006) and equation 17, this enhancement is anticipated to further increase significantly with  $Pe$ . These results were achieved with window opening  $\Delta=\pi/4$ , which is found to

be universally optimal for Newtonian fluids (Metcalf et al 2006). Experimental investigation has shown this is not the case for non-Newtonian and specifically yield stress fluids, hence further improvements are possible with further computation.

Our results are an example of the ability of chaotic advection to address difficult transport problems involving non-Newtonian fluids and indicate prospects for design and construction of low energy transport enhancement devices. In such applications optimisation of the control parameters is of paramount importance; this is facilitated by the so-called *composite spectral method* (Lester et al 2006a). This method can be applied to industrially relevant problems with minimal computational. In contrast, traditional methods are too costly to explore  $\mathbf{Q}$  to the required resolution.

## REFERENCES

- METCALFE, G., RUDMAN, M., BRYDON, A., GRAHAM, L. J. W. and HAMILTON, R., 2006, "Composing Chaos: An Experimental and Numerical Study of an Open Duct Mixing Flow", *AIChE J.*, **52**, 1, 9-28.
- LESTER, D. R., METCALFE, G., RUDMAN, M. and BLACKBURN, H., 2006a, "Global Parametric Solutions of Scalar Transport in Flows with Symmetries", Submitted, *Chaos*
- LESTER, D. R., METCALFE, G. and RUDMAN, M., 2006b, "Prospects for Efficient Enhanced Heat Transfer in an Open Chaotic Flow", *13th Ann. Int. Heat Trans. Conf.*, Sydney, Australia, August 13-18.
- LIU, W. and HALLER, G., 2003, "Strange Eigenmodes and Decay of Variance in the Mixing of Diffusive Tracers", *Physica D*, **188**, 1-39
- PIERREHUMBERT, R. T., 1994, "Tracer Microstructure in the Large-Eddy Dominated Regime", *Chaos*, **4**, 6, 1091-1110
- SPEETJENS, M., METCALFE, G. and RUDMAN, M., 2006, "Topological Mixing Study of non-Newtonian Duct Flows", Accepted, *Phys. Fluid.*